

REPORT DOCUMENTATION PAGE			Form Approved OMB No. 0704-0188	
Public reporting burden for this collection of information is estimated to average 1 hour per response, including the time for reviewing instructions, searching existing data sources, gathering and maintaining the data needed, and completing and reviewing the collection of information. Send comments regarding this burden estimate or any other aspect of this collection of information, including suggestions for reducing this burden, to Washington Headquarters Services, Directorate for Information Operations and Reports, 1215 Jefferson Davis Highway, Suite 1204, Arlington, VA 22202-4302, and to the Office of Management and Budget, Paperwork Reduction Project (0704-0188), Washington, DC 20503.				
1. AGENCY USE ONLY (Leave blank)	2. REPORT DATE Nov. 1, 1996	3. REPORT TYPE AND DATES COVERED 9/1/93-8/31/96		
4. TITLE AND SUBTITLE  Probing Solar Convection		5. FUNDING NUMBERS  G-F49620-93-1-0386 3484/YS		
6. AUTHOR(S)  Philip R. Goode				
7. PERFORMING ORGANIZATION NAME(S) AND ADDRESS(ES) New Jersey Institute of Technology Office of Sponsored Projects 323 Martin Luther King Blvd. Newark, New Jersey 07102		8. PERFORMING ORGANIZATION REPORT NUMBER		
9. SPONSORING/MONITORING AGENCY NAME(S) AND ADDRESS(ES)  AFOSR/PKA 110 Duncan Avenue Suite 115 Bolling AFB, Washington DC, 20332-0001		10. SPONSORING/MONITORING AGENCY REPORT NUMBER		
11. SUPPLEMENTARY NOTES				
12a. DISTRIBUTION/AVAILABILITY STATEMENT DISTRIBUTION UNLIMITED		12b. DISTRIBUTION CODE DISTRIBUTION STATEMENT A Approved for public release Distribution Unlimited		
13. ABSTRACT (Maximum 200 words)  This grant was used to support the MS and post-MS studies of Tom Spirock and Elliotte Harold. Mr. Harold studied data on acoustic event on the the Sun. From this, we learned that sunquakes, which enable us to seismically probe the inside of the Sun, have an unexpected source. We discovered that the quakes are caused by a catastrophic cooling and collapse of isolated, small regions of the Sun's surface. It had been widely believed that these quakes were caused by the steady drumming of material rising to the solar surface. Mr. Spirock developed a robotic, computer controlled arm for his thesis. This work represented a significant expertise in building instruments and using computers to control them.				
14. SUBJECT TERMS		15. NUMBER OF PAGES 14		
		16. PRICE CODE		
17. SECURITY CLASSIFICATION OF REPORT UN	18. SECURITY CLASSIFICATION OF THIS PAGE UNCLASSIFIED	19. SECURITY CLASSIFICATION OF ABSTRACT UNCLASSIFIED	20. LIMITATION OF ABSTRACT UNLIMITED	

NSN 7540-01-280-5500

Standard Form 298 (Rev. 2-89)  
Prescribed by ANSI Std. Z39-18  
298-102

[DTIC QUALITY INSPECTED 3]

## **FINAL REPORT**

This report is on G-F49620-93-1-0386. Section I describes the work of Elliotte Harold which is largely contained in a paper by Rimmele, Goode, Harold and Stebbins (Astrophysical Journal Letters 444, L119, 1995). The description of the work of Spirock is taken from his MS thesis. The MS theses of both are available in the NJIT library.

### **Section 1: Dark Lanes in Granulation & Excitation of Solar Oscillations**

We made simultaneous high resolution observations of the Sun's granulation and solar acoustic events in the photosphere. We found that the acoustic events, which are a local by-product of the excitations of solar oscillations occur preferentially in the dark, intergranular lanes. At the site of a typical acoustic event the local granulation becomes darker over several minutes leading up to the event with a further, abrupt darkening immediately preceding the peak of the event. Further, the stronger the acoustic event the darker the granulation. Thus, the excitation of solar oscillations seems more closely associated with the rapid cooling occurring in the upper convection layer, rather than the overshooting of turbulent convection itself.

Earthquakes shake the Earth allowing one to seismically sound our planet's interior. In an analogous way, sunquakes enable a sounding of the solar interior. The two kinds of quakes are also alike in that both are near surface phenomena. However, sunquakes are

19971006 005

DTIC QUALITY INSPECTED 8

always occurring somewhere on the Sun so that energy is being continuously fed to the Sun's resonant modes so that one, in principle, could continuously sound the Sun. From the global solar seismic data, we have learned what we know about the Sun's interior. This is true even though, unlike earthquakes, the precise origin of sunquakes has been shrouded in mystery.

We have made high resolution observations of the Sun in which we identify individual sunquakes and see the power from the quakes being pumped into the resonant modes of vibration of the Sun. We speculate on the local seismic potential of these acoustic events.

The resonant or normal modes of vibration of the Sun have taught us how to tune our models of the solar interior so that the seismic model of the Sun's pressure and density differs from that of our best theoretical model by only a few parts in a thousand throughout the Sun's interior. We have also been taught that the solar interior rotates a rate close to that of the surface. In detail, we now know that the outer quarter of the Sun rotates in about 25 days at the equator and 35 days near the poles with a gradual transition in between. This differential rate is indistinguishable from that Lord Carrington measured for the Sun's surface more than 100 years ago. There is also no evidence of differential rotation beneath the Sun's convection zone.

It is widely agreed that the Sun's global modes of vibration are excited near the Sun's surface as a part of the process in which convection stops being an efficient mechanism of energy transport. Looking at the solar surface in white light, one sees a granular structure

characterized by bright granules surrounded by dark lanes. The granules are about 1" (700 km) in diameter and the lanes are somewhat narrower. The bright granules are caused by a convective overshooting of warmer fluid from below into the non-convective called the solar photosphere. The sunlight we see comes from the photosphere. The heuristic picture is that as the overshooting element cools its fluid flows outward from its center and the dark lane is the downflow of the cooled fluid. Until recently, it was widely believed that this deceleration of the upgoing granules induced a steady drumming that fed the resonant acoustic modes. However, in the work with Mr. Harold, we observed that there are acoustic events which they associated with the excitation of solar oscillations. These events originate in the dark inter-granular lanes. Furthermore, we observed that the acoustic events were preceded by a greater darkening of an already dark lane, and, temporally, on the leading edge of the acoustic event there is a further, more abrupt darkening. From this, we suggested that the excitation of the resonant modes was caused by the occasional, catastrophic cooling and collapse of the lanes. However, they failed to show a causal link between the acoustic events and the resonant modes of vibration of the Sun.

Our observations were made at the Vacuum Tower Telescope of the National Solar Observatory in Sunspot, New Mexico. The dataset discussed here is from Sept. 5, 1994. The data and the reduction of it are described in detail in our Astrophysical Journal Letters paper (Rimmele, et al. 1995). One of our basic observational problems was to distinguish the acoustic event power from the dominant resonant mode power. To distinguish the

two in our field of view (60"x60" patch of quiet Sun near disk center), we measured the velocity as a function of altitude in the photosphere in our field of view ( for 65 min) by observing the Doppler shift in the 543.4 nm Fe I absorption line. The Doppler shift as a function of depth in the line corresponds to the velocity as a function of altitude in the atmosphere the line spans. With this information, we can distinguish between acoustic events and normal modes because the normal modes are very nearly evanescent in the photosphere, but the acoustic events are not. In 1909, Lamb first idealized the description of an acoustic event by considering the response of a stably stratified isothermal atmosphere to a thumping from below. He showed that the acoustic front passing outward would be followed by an oscillating wake which is an outgoing traveling wave. In a uniform atmosphere, there would be no wake. After the thumping ceases, the amplitude of the wake in the stratified atmosphere goes to zero, while its phase speed becomes very large and the wave frequency goes to that of the acoustic cut-off. In the solar photosphere, which is not quite isothermal, the outgoing wave is followed by a reflected wave. The combination of the outgoing wave followed by an ingoing wave (with a time lag of about four to five minutes) at some place in the field of view distinguishes power from an acoustic event from that of a normal mode which should show only a minimal, dissipative phase change with altitude. With this, we were able to cleanly distinguish acoustic events from oscillations and then determine the power in the events.

Since our field of view is typical of the Sun, we find that the power expended in the events is comparable to that required to power the solar oscillations. This is the first time such a power source has been found.

## **Sections II: A DIGITAL SIGNAL PROCESSOR BASED OPTICAL POSITION SENSOR AND ITS APPLICATION TO FLEXIBLE BEAM CONTROL**

### **ABSTRACT**

A Digital Signal Processor (DSP) based optical position sensor was developed. The sensor system consists of the following components: 1) Analog electronics, 2) The DSP based synchronous demodulation software, 3) PC based interface software which samples and saves the data, and 4) PC based control codes for a flexible beam experiment.

The ability of the system to determine the distance from the optical sensor to the power modulated light source was assessed by the following tests: 1) A stationary drift test to evaluate the system's noise, 2) A short-range test to determine the resolution of the optical sensor over a 25mm range and, 3) A long-range test to evaluate the ability of the system to predict the location of the optical sensor over a 600mm range. It was found that the resolution of the system is approximately 0.5mm for the short range test and 5mm for the long range test.

Finally, the sensor was deployed for the position feedback of a flexible beam experiment. Performance indices used to evaluate the response of the system were: 1) The sum of the squared position error, 2) The final steady state position error of the end of the flexible beam, and 3) The 5% settling time of the flexible beam. A number of control laws were evaluated and it was determined that a variable PID controller produced the best overall performance. The system can consistently position the end of the flexible beam from a +/- 20cm to within 5mm of the command position in approximately 8 seconds with a properly tuned controller.

## **CHAPTER 1**

### **INTRODUCTION**

In this thesis work, an optical position sensor has been designed and implemented. A number of tests were performed to characterize the drift, short-range, and long-range properties. The system was then deployed in a flexible beam control experiment.

#### **1.1 Introduction**

The purpose of the project is to design and build an optical position sensor and to apply this sensor in motion control systems. The sensor's operation is based on the inverse square law property of light propagation which is used to derive the distance between a power-modulated laser diode and a light intensity sensor.

A Digital Signal Processor (DSP) is used to 1) Power-modulate the laser diode, 2) Sample the light intensity signal from the optical sensor, 3) Perform synchronous demodulation on the intensity signal, and 4) Pass the data to the host PC for further calculations. To perform the stated functions of the system both the analog electronics; which power the laser diode and pre-process the signals from the light intensity sensors, and the software; which performs the synchronous demodulation and power-modulate the laser diode, have been developed.

## 1.2 Signal Flow and Description of Variables

In this section, a brief overview of the system configuration and pertinent signals is provided. All subsequent discussions will be referenced to the diagrams and table in this section. Block diagrams of the signal flow are shown in Figure 1.1 and Figure 1.2. A description of the signals appears in Table 1.1.

Figure 1.1 is a block diagram of sensor system and DSP signal flow. The signals from the analog electronics are sampled at 10KHz by the A/D (analog to digital converter). Synchronous demodulation is then performed on the sampled signals to extract their amplitudes which correspond to the non-normalized intensity signals from the sensor modules. The average values of the amplitudes are stored in the external memory where it can be accessed by the host PC for further analysis.

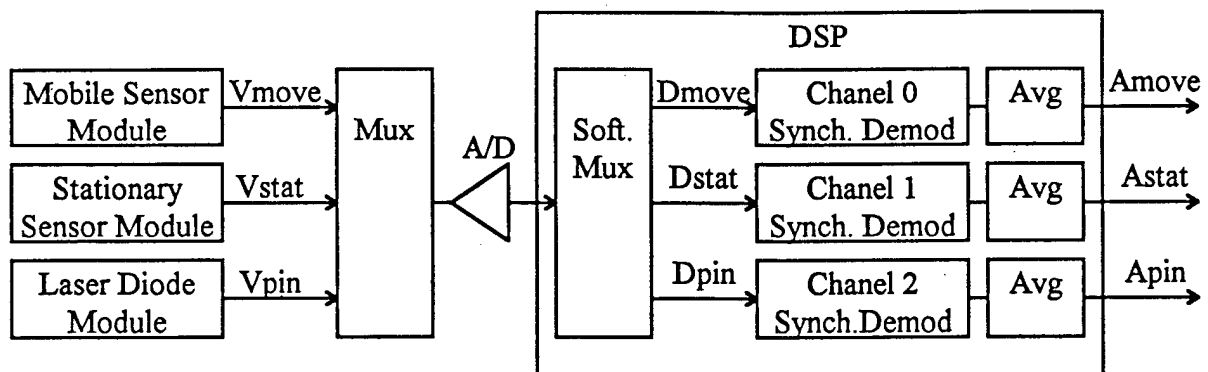
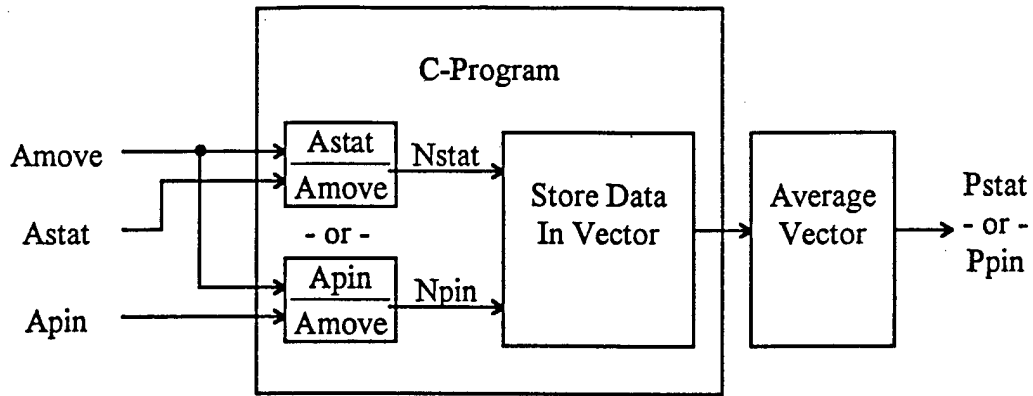


Figure 1.1 Block diagram of sensor system and DSP signal flow.

Figure 1.2 describes the signal flow in the host PC. The output data from the DSP are stored in dual ported external memory. Post processing of the sensor data, such as normalization and interpolation is performed by a C-program executed in the host PC.





**Figure 1.2** Block diagram of software signal flow in the host PC.

**Table 1.1** Descriptions of Signals

Signal	Description
Vmove	The analog sine wave output from the mobile sensor module.
Vstat	The analog sine wave output from the stationary sensor module.
Vpin	The analog signal from the laser diode feedback circuit.
Dmove	The 10KHz sampled Vmove signal.
Dstat	The 10KHz sampled Vstat signal.
Dpin	The 10KHz sampled Vpin signal.
Amove	Average of the Non-normalized mobile sensor module's position.
Astat	Average of the Non-normalized stationary sensor module's position.
Apin	Average of the laser diode's output signal.
Nstat	Position signal normalized by the stationary sensor module.
Npin	Position signal normalized by the laser diode's feedback signal.
Pstat	Time average of the Nstat signal.
Ppin	Time average of the Npin signal.

### **1.3 Thesis Organization**

The organization of this thesis is as follows: Chapter Two describes the hardware development such as the optical sensor modules, the laser-diode module, data sampling schemes, the one-dimensional testing setup and the application of the sensor module as the position sensor for a flexible beam experiment. Chapter Three describes the software development such as the DSP assembly language program which performs synchronous demodulation on the optical sensor output signals and the C-programs, which are executed on the host PC, which save the position data from the DSP and execute the control program for the flexible beam experiment. Chapter Four characterizes the performance of the sensor system. Finally, Chapter Five describes the application of the system to the flexible beam experiment.

## CHAPTER 6

### CONCLUSIONS

In this thesis work, an optical position sensor has been designed and implemented

#### 6.1 Sensor Module Characterization

The characteristics of the sensor module were analyzed in Chapter 4 using various standard test procedures such as drift stability, short-range repeatability, and long-range repeatability. A summary of these test results are tabulated in Table 6.1 below. Based on these results, the following conclusions are now drawn:

**Table 6.1** Summary of test results from Chapter 4.

Test	Location Repeatability (+/- mm)	Range (mm)	Resolution (mm)
Short range w/ Pstat	0.02	25.4	0.5
Long range w/ Pstat	2	600	5
Long range w/ Ppin	2	600	4

1) The system can predict the location of the mobile sensor module to an accuracy of 0.5 mm when used in the short-range test where the known position repeatability is 0.02 mm (Refer to Section 4.3 for a review of the short-range test).

2) The system can predict the location of the mobile sensor module to an accuracy of 5 mm when used in the long-range test where the known position repeatability is approximately

2 mm and the stationary sensor module output is used as the normalization signal (Refer to Section 4.4 for a review of the long-range test when the stationary sensor module output is used as the normalization signal).

3) The system can predict the location of the mobile sensor module to an accuracy of 4 mm when used in the long-range test where the known position repeatability is approximately 2 mm and the feedback signal from the laser diode's output power is used as the normalization signal (Refer to Section 4.5 for a review of the long-range test when the feedback signal from the laser diode's output power is used as the normalization signal).

## **6.2 Flexible Beam Experiment**

Based on the test results of the flexible beam experiment discussed in Chapter 5, which tested the ability of the control system (Section 2.7) to position the flexible beam to the command position when the position feedback signal is produced by the mobile sensor module attached to the end of the flexible beam, the following conclusion can be made: The system can consistently position the end of the flexible beam to within 5 mm of the command position in approximately 8 seconds when used with a properly tuned PID controller.

Also note that there is an advantage of using a microprocessor based control system over an analog-circuit based control system for the following reasons: 1) The properties of the control system can be easily changed by editing the control software rather than making changes to analog circuit components, 2) The coefficient values in the control software are stable over time where the component values of an analog circuit can change due to environmental conditions and over time, and 3) Complex logic and arithmetic operations can be easily implemented by a microprocessor.

### 6.3 Future Improvements

The following is a listing and discussion of proposed future improvements to increase the ability of the system to predict the location of the mobile sensor module:

1) By far the greatest improvement to the system would be to incorporate the Time Sampling scheme, as discussed in Section 2.5.1, which would require the use of a floating point processor. This would eliminate the need for the analog electronics required to pre-process the signal from the sensor modules and enable the DSP to sample to time between the data pulses from the TSL220 light sensor to an accuracy of 0.1 $\mu$ S.

2) The use of a floating point processor would also improve the realization of the digital filters, which can only be approximated with a fixed point processor.

3) Since the output frequency of the TSL220 light sensor is determined by an external capacitor for a given incident light intensity, it is critically important that the value of the capacitor remain very stable. This can either be accomplished with an active monitor and compensator for the capacitance or a forthcoming version of the TSL220 light sensor that no longer requires an external capacitor to control the output frequency.

4) All digital monitoring of the laser diode's output power feedback signal which would remove the need for the analog highpass filter circuit (Figure 2.7) and improve the stability of the monitored feedback signal.

5) A variable lens setup which can create either a rapidly diverging cone of light from the laser diode which would optimize the system for the short range discussed in Section 4.3 or a slowly diverging cone of light which would optimize the system for the long range tests discussed in Sections 4.4 and 4.5.

6) Further optimization of the control program for the flexible beam experiment and the incorporation of the dynamics of the flexible beam to realize a compensator in the control program.

7) The use of multiple sensor modules on the flexible beam to monitor and compensate for the flexure in the flexible beam.